



Air-coupled ultrasound detection of natural defects in wood using ferroelectret and piezoelectric sensors

M. Tiitta¹ · V. Tiitta¹ · M. Gaal² · J. Heikkinen¹ · R. Lappalainen¹ · L. Tomppo¹

Received: 27 December 2019 / Published online: 28 May 2020
© The Author(s) 2020

Abstract

Air-coupled ultrasound was used for assessing natural defects in wood boards by through-transmission scanning measurements. Gas matrix piezoelectric (GMP) and ferroelectret (FE) transducers were studied. The study also included tests with additional bias voltage with the ferroelectret receivers. Signal analyses, analyses of the measurement dynamics and statistical analyses of the signal parameters were conducted. After the measurement series, the samples were cut from the measurement regions and the defects were analyzed visually from the cross sections. The ultrasound responses were compared with the results of the visual examination of the cross sections. With the additional bias voltage, the ferroelectret measurement showed increased signal-to-noise ratio, which is especially important for air-coupled measurement of high-attenuation materials like wood. When comparing the defect response of GMP and FE sensors, it was found that FE sensors had more sensitive dynamic range, resulting from better *s/n* ratio and short response pulse. Classification test was made to test the possibility of detecting defects in sound wood. Machine learning methods including decision trees, *k*-nearest neighbor and support vector machine were used. The classification accuracy varied between 72 and 77% in the tests. All the tested machine learning methods could be used efficiently for the classification.

Introduction

Ultrasound and other acoustic techniques are widely used as nondestructive testing techniques for the detection of internal defects and strength determination of wood (Bucur 2003, 2005, 2011; Chimenti 2014; Fang et al. 2017; Ross and Pellerin 2002;

✉ M. Tiitta
markku.tiitta@uef.fi

¹ Department of Applied Physics, University of Eastern Finland, PO Box 1627, 70211 Kuopio, Finland

² Federal Institute for Materials Research and Testing (BAM), Unter den Eichen 87, 12205 Berlin, Germany

Solodov et al. 2004). Density, wood structure and different types of discontinuities exert various effects on ultrasound propagation. Wood defects affect the mechanical properties of wood and thus the propagation of ultrasound signal in wood. For example, delaminations cause additional reflections, which reduce the transmission signal. Various studies have been conducted to evaluate defects by ultrasound (Kabir et al. 2002; Schmoldt et al. 1994; Tiitta 2006; Tiitta et al. 1998, 2001, 2017; Tomppo 2013; van Dyk and Rice 2005). Unsound knots, decay, bark pockets, holes and wane cause variation in ultrasound signal compared to clear wood even in fresh-cut high moisture content (MC) state (Kabir et al. 2002). Internal checks and surface cracks increase the ultrasound transmission time perpendicular to grain (Fuller et al. 1994). In addition, the bacterially infected sections of wetwood increase the stress wave travel time (Verkasalo et al. 1993). Presumably, the internal cracking in wood causes scattering of the ultrasound, whereas wetwood increases the viscoelastic damping, both resulting in attenuated sound signals (Schafer et al. 1999).

The development of air-coupled ultrasound (ACU) techniques (Bhardwaj 2004) has made the ultrasound method more feasible for online industrial applications. Recent ACU techniques include ferroelectric sensors with and without additional bias voltage (Gaal et al. 2016a, b, 2019; Vössing et al. 2018; Vössing and Niederleithinger 2018). Online wood MC measurement based on ACU has been proposed (Vun et al. 2008), and density and defects in wood have been studied using ACU (Marchetti et al. 2004). In addition, through-transmission ACU has been utilized in the detection of cracks in wood and thermally modified timber (TMT) (Gan et al. 2005; Tomppo et al. 2016), delamination in wood (Bucur 2010, 2011) and in glulam beams of an arbitrary number of lamellas up to 500 mm thickness (Sanabria 2012; Sanabria et al. 2013). In wood-based panels, both density and particle type affect ultrasound transmission (Vun and Bhardwaj 2004; Hilbers et al. 2012).

This study is part of a research project, where new nondestructive methods were tested and developed for wood analyses. Oak, spruce and TMT spruce sawn timber samples were measured using ACU under laboratory conditions to find out relations between defects of wood and the responses. A substantial number of studies has been conducted to detect artificial defects in wood and wood products using ACU. In this study, the natural defects included knots and cracks from wood processing and tree growth. The objective of the study was to evaluate and compare novel ACU sensors for the detection of the natural defects in wood. Machine learning techniques were used for the defect classification.

Materials and methods

Table 1 shows the properties and defects of examined wood board samples including hardwood, softwood and thermally modified timber (TMT). After the ultrasound tests, all the samples were cut to 10 mm slices for visual analysis of growth ring angle (GRA) and defects. All samples included regions free of defects and regions with defects. Analyzed defects include cracks, knots, resin pockets, ring shake and compression wood. Analyses were made by naked eye.

Table 1 Examined samples including visually detected defects from cross sections and surface

| Species | Type | Defects | Sample dimension (mm) | <i>N</i> |
|---------|--------------|--|-----------------------|----------|
| Red Oak | Hardwood | Cracks | 700×92×23 | 3 |
| Spruce | Softwood | Knots, compression wood | 700×110×30 | 2 |
| Spruce | Softwood | End crack, knots, resin pocket | 630×247×51 | 1 |
| Spruce | TMT-softwood | Resin pockets, cracks, knots, ring shake | (645–700)×130×38 | 3 |

N is the number of measured boards

The ultrasound measurements were performed using the air-coupled ultrasonic system USPC 4000 AirTech from Hillger NDT GmbH (Braunschweig, Germany, Fig. 1), and pulse length was adjusted to the resonance frequency f , that means equal to $1/(2f)$. The sample was placed between the transmitter and the receiver, which were synchronized and moved over the surface. The distance between transmitter and wood varied between 30 and 70 mm, and the distance between receiver and wood varied between 40 and 55 mm, always adjusted to the focusing distance of the applied transducers. C-scan images from signal height and the time of flight (ToF) were displayed while scanning.

GMP and FE transducers differed in terms of frequency, apparatus diameter and focusing (Table 2). The studied frequency range was 100–200 kHz, and the sensor diameter range was 19–27 mm (Gaal et al. 2016a). The GMP transmitters were excited with a unipolar square pulse with 200 V amplitude, while the FE transmitters were excited with 1.8 kV unipolar pulses, so that the electrostatic compression of this cellular material makes a significant contribution to its vibration (Döring et al. 2010, 2012). In the last part of the scanning tests when scanning the high-attenuation TMT samples, the FE receiver was connected to a high-voltage bias unit providing 2 kV DC voltage, which increased the sensitivity of the receiver (Gaal

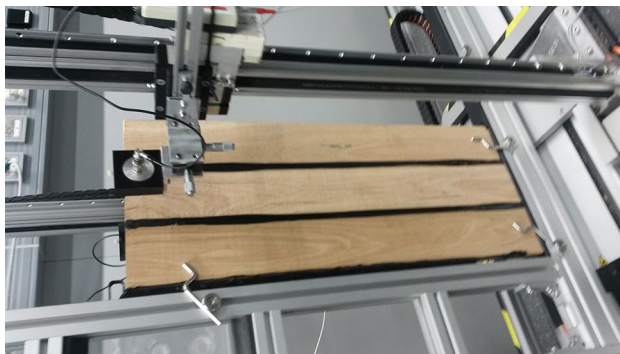


Fig. 1 Scanning measurement system. The scanning was made in 2 mm pixel size. The samples were placed between the transmitter and receiver. Samples requiring the same setup of the ultrasonic equipment were connected with a glue. Ultrasound propagation direction was radial/tangential. The red oak samples are shown

Table 2 Tested sensor models

| Transducer pairs | Frequency (kHz) | Active diameter (mm) |
|------------------------|-----------------|----------------------|
| CPP 710/709 A27 | 100 | 27 |
| Ultran NCG100-D25 | 100 | 25 |
| CPP 708/707 A27 | 130 | 27 |
| Ultran NCT200-D25-P150 | 142 | 25 |
| CPP 722/721 A27 | 200 | 27 |
| Ultran NCG200-D19 | 200 | 19 |

Ultran sensors are GMP sensors from The Ultran Group (State College, PA, USA), while CPP sensors are FE sensors made of cellular polypropylene and developed at BAM

et al. 2019). This sensitivity increase can be understood if the FE is modeled as a capacitor and the FE receiver as a capacitive microphone. The internal polarization of the voids in FE has the effect of bias voltage in a capacitive microphone, which is responsible for piezoelectric properties of FE. External bias voltage with the same polarity increases the total bias voltage and thus the sensitivity of the FE receiver.

Data analysis

Classification tests were made using three different classifiers: decision trees (DT), *k*-nearest neighbor (KNN) and support vector machines (SVM) (Fig. 2). The classification was tested and compared by using training and testing sets. The input from the training set was fed into a classifier, and the classifier was trained. After the training, the testing set was fed into the trained classifier and the correctness of the operation was determined. Cross-validation was used for each of the models because the number of tested samples was relatively small (420). Cross-validation gives more generalized results and prevents overfitting of the predicted model because the accuracy is based on the whole dataset. 50-times cross-validation was used, so data were split to 50 different training and test sets, and accuracy of the model is the mean accuracy from all the trained models. The training time varied from 2 to 3 s. The tests were made using Matlab2018b and Classification Learner app (The MathWorks, Inc., Natick, MA, USA).

Decision tree is a nonparametric classifier. It builds a tree model based on the input of the data. The root of the tree is the entire population of the data, and each leaf presents different classification result of the data. Nodes of the tree are called the decision nodes, and they represent different input values. The output leaf is selected based on these decision nodes.

K-nearest neighbor classifier is a nonparametric classifier. The training set for each class represents a class, and the unknown pattern from the testing set is classified by finding the nearest neighbors from the sets of training patterns. Statistically, more reliable results can be achieved by using more than one nearest neighbor. In

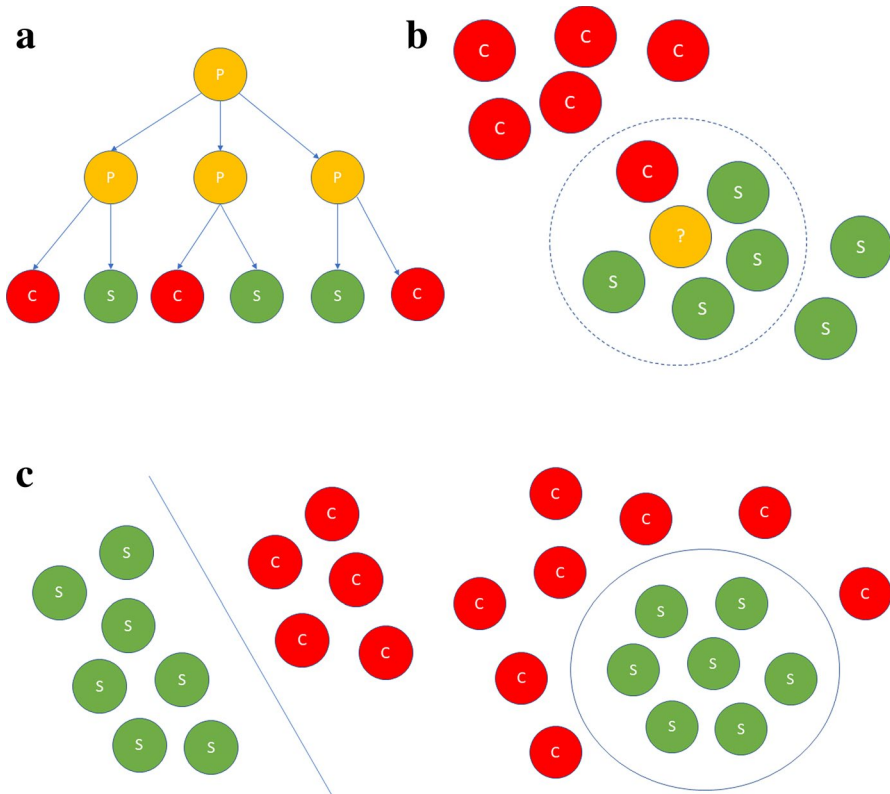


Fig. 2 Principle of the classifiers: **a** decision trees, **b** k -nearest neighbor, **c** support vector machine

KNN, the unknown pattern is placed in a class with most of the k -nearest neighbors in the training set.

Support vector machine is a nonparametric classifier. It creates hyperplane, which separates dataset to different classes. This hyperplane maximizes the margin between the classes, and it can be linear or nonlinear separable. Support vectors are datapoints, which affect the position and orientation of the hyperplane.

Results and discussion

Cracks, growth ring angle (GRA: T —tangential, R —radial), resin pockets and knots were analyzed for their effects on air-coupled ultrasonic signal propagation in wood. GMP and FE sensors were compared. The effect of additional bias voltage with the FE sensors was analyzed too. Detected and non-detected defects are shown in Fig. 3. Figure 4 shows a C-scan image measured by FE 100 kHz sensors. Three boards were attached together with some glue for the scanning (Fig. 1). The cracks inside the boards were visible in the C-scan image, as well

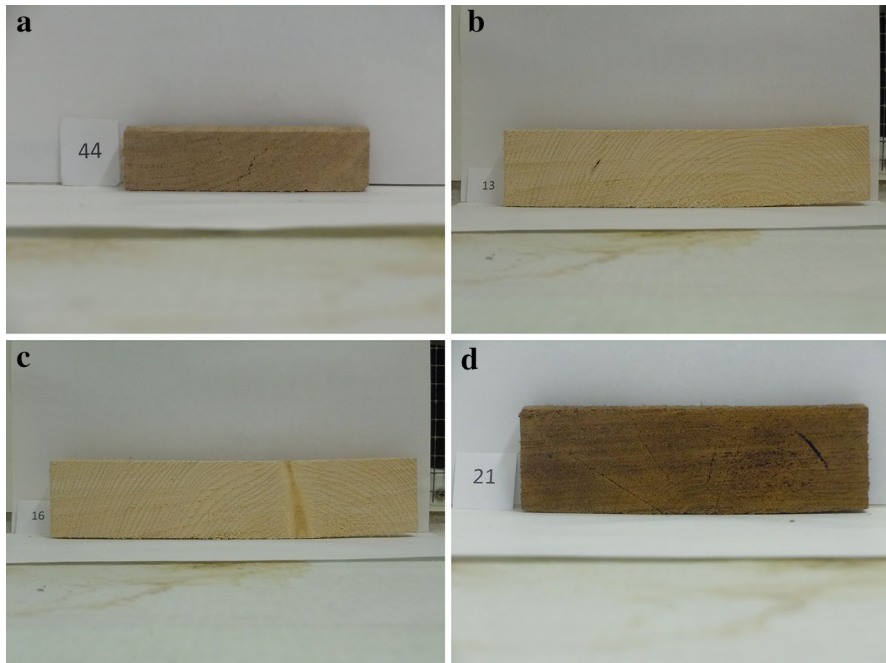


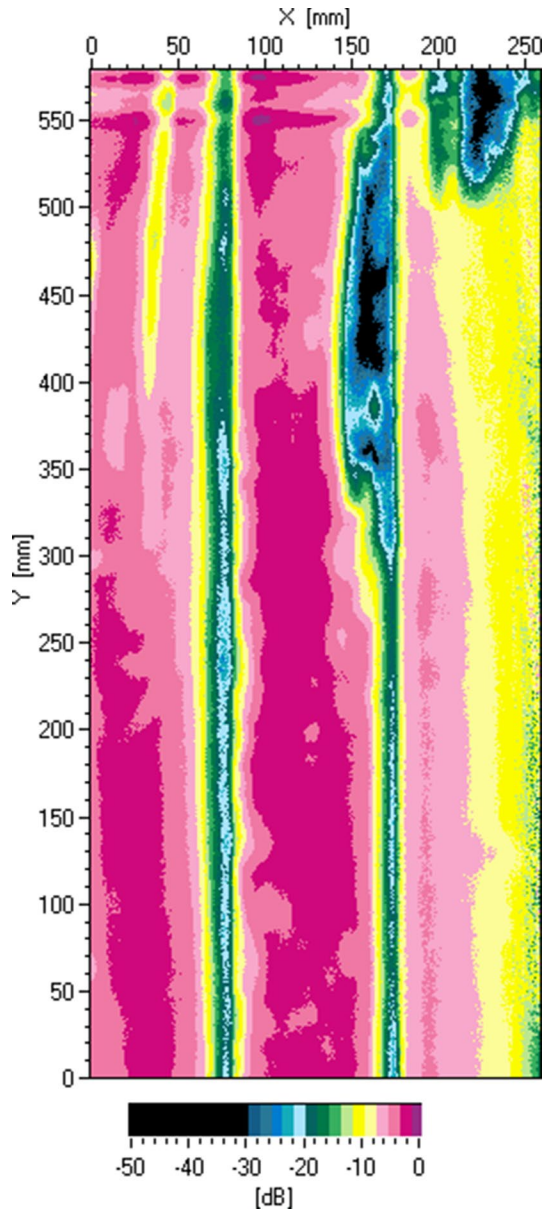
Fig. 3 Detected and non-detected defects: **a** detected internal crack, red oak, **b** non-detected small resin pocket, **c** detected knot, **d** detected cracks and resin pocket, TMT spruce

as the highly reflective glue between the boards. The response of a crack (Fig. 3a) can be seen in C-scan at positions ($x=30$ mm, $y=400$ – 600 mm). Examples of signals and defect responses are shown in Figs. 5 and 6. Decreased amplitude of ultrasound with the TMT samples is shown as increased noise level, which could be seen with all the tested sensors.

One of the basic analyses to investigate the ultrasound responses of defects is to compare the signals measured through defect to the signals measured from defect-free region near the defect (Table 3).

The effect of GRA was evident (Table 3). In radial direction, all sensors had clear response with the studied defects. Because of the low amplitude in sound *R/T* region, the effect of a defect is clearly smaller than when measuring a wood region with radial GRA. The effect can be seen with all sensor types. The used frequency affected the response. For the same wood type, the lowest tested frequency had higher amplitude than the highest frequency. The effect was compensated by adjusting receiver amplification to get dynamically good signals levels. Typically, it is possible to detect smaller defects with smaller diameter transducer and higher frequency because of the narrower beam. The rule of thumb is that defects may be detected from half the size of the transmitter/receiver (Sanabria 2012). With the recent studies, even with a large sound field, very small defects could be found with small receivers using ACU-TR method (Marhenke et al. 2020). On the other hand, wood is very structured and non-uniform, which causes variation in the signal even

Fig. 4 C-scan attenuation (dB) image from the three red oak samples. FE 100 kHz sensors. The samples and sensors are shown in Fig. 1. The border lines between the samples are located at 75 mm and 170 mm at x -axis, and they are shown as low amplitude lines. Cracks were detected by 10–50 dB decrease in the signal compared to the surrounding sound wood. Cracks are shown at positions ($x=30\text{--}40$, $y=400\text{--}600$), ($x=150\text{--}160$, $y=300\text{--}550$) and ($x=215\text{--}250$, $y=530\text{--}600$) mm. The cracks detected by ultrasound corresponded to the visual findings from the cross sections



without defects. The ultrasound beam may be skewed inside the wood because of for example GRA or defects, which makes the analysis more complex.

All sensors detected the cracks in the oak samples and big cracks in TMT samples. For the spruce samples, some of the knots were detected. Small knots and small resin pockets within R/T region were not detected with any sensor, but big knots and knots in radial region were detected (Fig. 7); crack oriented parallel with ultrasound

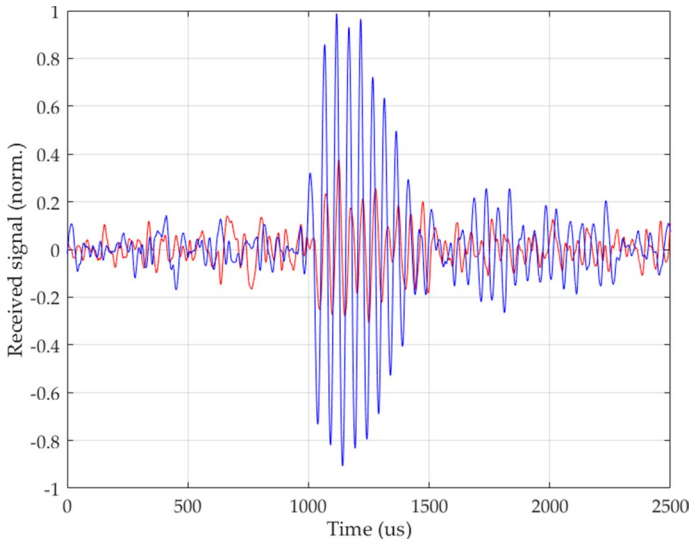


Fig. 5 Example of a response. FE 200 kHz sensor pair with receiver bias. Through-transmission signal through TMT spruce; high amplitude (blue)—signal through sound wood; low amplitude (red)—signal through resin pocket (Fig. 3d) (color figure online)

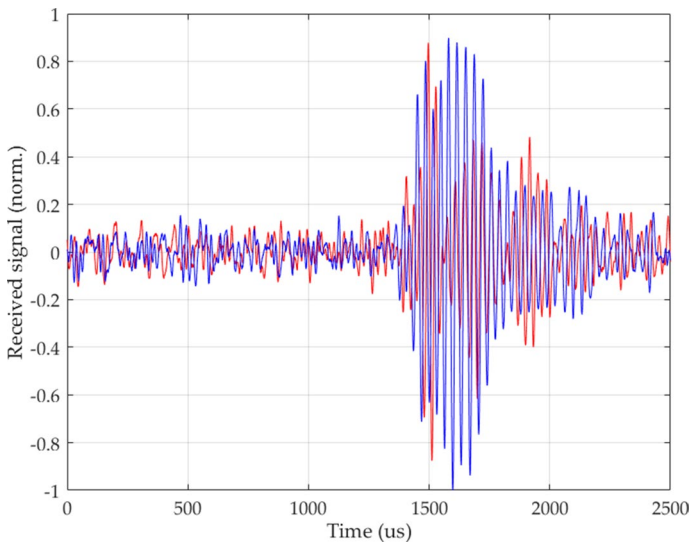


Fig. 6 Example of a response. GMP 200 kHz sensor; spruce sample (thickness 51 mm), radial direction through-transmission signal through spruce S3; high amplitude (blue)—signal through sound wood; low amplitude (red)—signal through the knot (Fig. 3c) (color figure online)

Table 3 Change in amplitude (dB) between sound and defect region (cracks and knots)

| Sensor | Red oak <i>R/T</i> | Red oak <i>R</i> | TMT <i>R</i> | Spruce <i>R</i> |
|--------------------------------|--------------------|------------------|--------------|-----------------|
| CPP710 100 kHz nb ^a | − 8.9 | − 23.1 | − 15.4 | − 11.4 |
| CPP708 128 kHz nb ^a | − 9.4 | − 23.1 | − 14.0 | − 11.4 |
| CPP221 200 kHz nb ^a | − 6.7 | − 24.4 | − 13.6 | − 9.6 |
| NCG100-D25 100 kHz | − 4.4 | − 23.1 | − 3.3 | − 23.1 |
| NCT200-D25-P150 | − 8.0 | − 19.2 | − 8.0 | − 8.0 |
| NCG200-D19 200 kHz | − 8.0 | − 24.4 | − 6.0 | − 20.9 |

GRA *R* versus *R/T*. Red oak and TMT samples contained cracks, whereas spruce samples contained knots

^aNon-biased

beam was not detected. The effect of GRA is clear, the highest amplitude is at nearly radial direction (GRA 2°, $x=150\text{--}180$ mm). The nearly tangential direction (GRA 63°, $x=0\text{--}20$ mm) has higher amplitude than GRA near 45° ($x=90\text{--}110$ mm).

With the TMT samples, the ultrasound response was poorer with all sensor types. Efficient detection of cracks and other defects was possible in radial GRA. Table 4 shows the results of the determined signal parameters at 200 kHz. Signal-to-noise ratio was the best with the biased FE sensor, but the difference between non-biased and biased FE sensor for detecting defects was quite small, and the difference was − 12 dB and − 13 dB for biased and non-biased sensor, respectively. With the FE sensors, the response of cracks was higher than with GMP sensors (− 7.2 dB). According to this study, the signal height is the best parameter indicating cracks, which is well in accordance with the previous study (Tomppo et al. 2014). The effect of cracks on ToF and frequency seemed to be nonlinear and the parameters were highly affected by the wood structure even more than cracks. When the signal is very poor, stable ToF measurement is very difficult because threshold values may affect the response and it is not possible to detect the first crossing with high precision. Besides the advantages of FE transducers, a few words should be said about their disadvantages. The main one is the loss of sensitivity when they are exposed to temperatures above 70 °C, when they partially lose their charge, or below about 0 °C, when they become stiffer and brittle. Another disadvantage is the mechanical sensitivity of the surface, which is deposited with 100 nm aluminum layer, which can easily be damaged. There are still no comprehensive studies on their long-term behavior. One FE transducer based on cellular polypropylene was in continuous use as a transmitter, excited with 2 kV square pulses with 100 Hz pulse repetition rate for 10 months, and it has shown a decrease in sensitivity of only 10%. However, it suffered a few electric breakthroughs, which damaged it locally. When using 1800 V, there were no breakthroughs recorded after repeated use.

GMP 200 sensor (NCT200-D25-P150) had a very unique frequency response. Though the frequency was near 200 kHz, the frequency spectra included two separate peaks. Thus, the frequency response changed a lot when moving sound region to cracked region. The response was highly affected by the crack type and orientation as well as the wood structure. Thus, it is difficult to use the parameter for stable

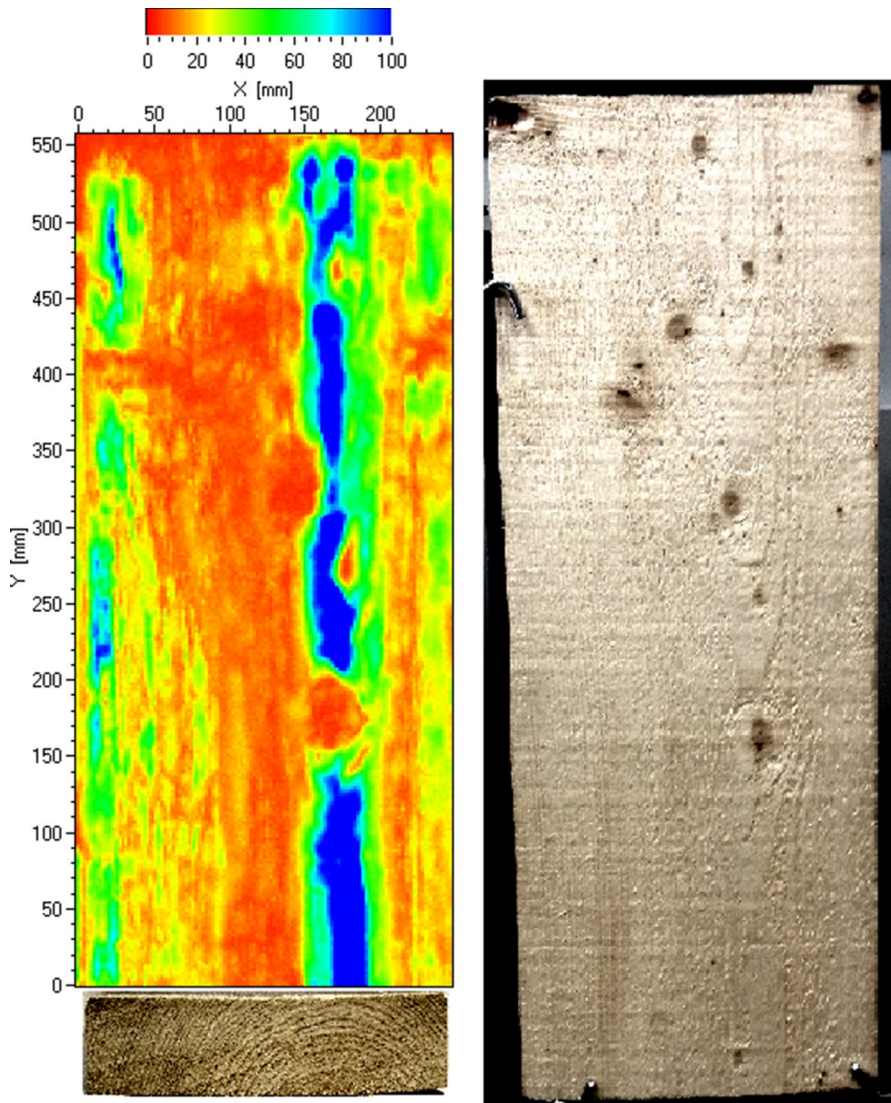


Fig. 7 C-scan amplitude (%) image from spruce (thickness 51 mm) using GMP 200 kHz (NCG200-D19) sensors. Visual analysis was made from surface and cross section samples. GRA varied from 63° (x : 0 mm) to 2° (x : 170 mm) to 42° (x : 250 mm). Visually detected knot location coordinates were [x (mm), y (mm)]: (28, 400); (115, 435); (116, 532); (138, 332); (160, 172); (160, 532); (170, 465); (212, 490) and (220, 420)

analysis. On the other hand, frequency may be used to distinguish different types of defects because it is known that for example decay is highly attenuating, especially the high frequencies compared to the low frequencies.

Three TMT-boards were tested with the three different classifiers using the 200 kHz FE sensors with bias. Boards were separated to four different pieces

Table 4 TMT-spruce analysis, 200 kHz sensors: mean, standard deviation (SD) and the difference between cracked and sound region

| Sensor pair | Good mean \pm SD | Crack mean \pm SD | Difference mean \pm SD |
|-----------------------------|--------------------|---------------------|--------------------------|
| <i>GMP 200 kHz</i> | | | |
| Signal height (dB) | -7.0 ± 1.4 | -14.2 ± 0.5 | -7.2 ± 1.5 |
| ToF (μ s) | 352.6 ± 4.1 | 355.4 ± 4.3 | 2.8 ± 5.9 |
| Freq. (kHz) | 166.8 ± 12.0 | 264.4 ± 21.8 | 97.6 ± 24.9 |
| <i>FE 200 kHz</i> | | | |
| Signal height (dB) | -10.4 ± 2.3 | -23.5 ± 0.7 | -13.1 ± 2.4 |
| ToF (μ s) | 248.6 ± 2.2 | 272.6 ± 3.1 | 24 ± 3.8 |
| Freq. (kHz) | 207.2 ± 3.4 | 207.6 ± 4.0 | 0.4 ± 5.2 |
| <i>FE 200 kHz with bias</i> | | | |
| Signal height (dB) | -3.5 ± 2.9 | -15.5 ± 1.2 | -12.0 ± 3.1 |
| ToF (μ s) | 363.5 ± 1.9 | 369.8 ± 1.6 | 6.3 ± 2.5 |
| Freq. (kHz) | 196.7 ± 1.7 | 176.2 ± 7.6 | -20.5 ± 7.8 |

All scans were conducted from the same region and the same samples: R6a, R6b and R6c (GRA R/T). Amplitude or signal height (dB), Time of Flight (ToF) and the peak frequency (Freq. kHz)

widthwise and 1 cm pieces lengthwise resulting in 152, 136 and 132 pieces. Thus, there were 420 pieces in total for the classification analysis. Statistics were calculated from amplitude, attenuation, time of flight and frequency from measured data. Minimum, median, maximum, mean and standard deviation values were used, and thus the total number of inputs for each of the parts is 20 (4×5). First, test was made with two different classes; sound and cracked areas. Total number of samples were 384. Table 5 shows the results of the classifiers:

Support vector machine gave the best results with 75.8% accuracy. The lowest accuracy was 71.9% with the decision trees. Table 6 shows the confusion tables from the trained models with knots.

The knots and cracked knots did not change the overall classification remarkably as the number of samples from the cracked knots, and knots was clearly smaller than in cracked and sound areas. Cracked knots were classified mainly as cracks and knots as no crack. All the tested machine learning methods worked well for the classification; no clear differences between the methods were found. All the parts were visually classified, and knot areas are usually much smaller than the cracked areas. Thus, if there is any error in position in visual analysis, the accuracy of detecting knots and cracked knots also is much lower than in cracked areas.

Table 5 Two-class classification accuracy without knots

| Model | N | Parameters | Classes | Accuracy (%) |
|-------|-----|------------|---------|--------------|
| KNN | 384 | 20 | 2 | 74.2 |
| SVM | 384 | 20 | 2 | 75.8 |
| DT | 384 | 20 | 2 | 71.9 |

Table 6 Classification results, confusion tables (cracked includes cracked knot and cracks; no crack includes sound wood and knots: (a) SVM classifier; (b) KNN classifier; (c) DT classifier; $N=420$)

| | No crack | Cracked | N |
|--------------------------------|------------|------------|------------|
| <i>(a) SVM: accuracy 73.6%</i> | | | |
| No crack | 205 | 56 | 261 |
| Cracked | 55 | 104 | 159 |
| <i>N</i> | 260 | 160 | 420 |
| <i>(b) KNN: accuracy 76.0%</i> | | | |
| No crack | 217 | 44 | 261 |
| Cracked | 57 | 102 | 159 |
| <i>N</i> | 274 | 146 | 420 |
| <i>(c) DT: accuracy 76.7%</i> | | | |
| No crack | 210 | 51 | 261 |
| Cracked | 47 | 112 | 159 |
| <i>N</i> | 257 | 163 | 420 |

Bold—correctly classified

The detection sensitivity and accuracy of air-coupled ultrasound depend for example on the frequency, sensitivity, size and focus of the sensors. For wood analyses, it is of utmost importance to understand the wood structure and its effect on ultrasound propagation. Defect detection is highly affected by the structure of wood, defect type and orientation. This study suggests that air-coupled ultrasound and machine learning may be efficiently used to detect natural defects in wood.

Conclusion

Cellular polypropylene FE and GMP transducers were used to detect natural defects in wood. The study included tests with additional bias voltage with the FE receivers. This study suggests that air-coupled ultrasound may be efficiently used to detect natural defects like cracks and cracked knots in wood though it seems obvious that it is not possible to distinguish small knots or cracks from sound wood because of ring angle variations without advanced multiple parameter analysis. Classification test was made to test the possibility of detecting defects from sound wood. The test was made using the 200 kHz FE sensors with bias resulting in high sensitivity and improved signal-to-noise ratio compared to other sensors. Machine learning methods including decision trees, k -nearest neighbor and support vector machine were used. When sound areas and areas with cracks including cracked knots were used in the classification analysis (two classes), it was possible to distinguish cracked areas from sound ones with 77% efficiency. The study showed the potential of using the novel FE sensors and machine learning to detect natural defects in wood.

Acknowledgements Open access funding provided by University of Eastern Finland (UEF) including Kuopio University Hospital. This study was partly funded by Business Finland (SEBI-Project 4619/31/2016), and the authors thank the steering group of the project for its guidance and fruitful discussions related to this study.

Compliance with ethical standards

Conflict of interest The authors declare no conflict of interest. The funder had no role in the design of the study; in the collection, analyses, or interpretation of data; in the writing of the manuscript, or in the decision to publish the results.

Open Access This article is licensed under a Creative Commons Attribution 4.0 International License, which permits use, sharing, adaptation, distribution and reproduction in any medium or format, as long as you give appropriate credit to the original author(s) and the source, provide a link to the Creative Commons licence, and indicate if changes were made. The images or other third party material in this article are included in the article's Creative Commons licence, unless indicated otherwise in a credit line to the material. If material is not included in the article's Creative Commons licence and your intended use is not permitted by statutory regulation or exceeds the permitted use, you will need to obtain permission directly from the copyright holder. To view a copy of this licence, visit <http://creativecommons.org/licenses/by/4.0/>.

References

- Bhardwaj MC (2004) High efficiency non-contact transducers and a very high coupling piezoelectric composite. In: Proceedings of 16th world conference on nondestructive testing, August 30th–September 3rd, Montreal, Canada
- Bucur V (2003) Nondestructive characterization and imaging of wood. Wood Science, Springer
- Bucur V (2005) Acoustics of wood. Springer Series in Wood Science. Springer, Berlin
- Bucur V (2010) Delamination detection in wood-based composites, a methodological review. In: Burgess M, Davey J, Don C, McMinn T (eds) Proceedings of 20th international congress on acoustics, ICA, August 23rd–27th, Sydney, Australia
- Bucur V (2011) Delamination in wood, wood products and wood-based composites, 1st edn. Springer, Dordrecht
- Chimenti DE (2014) Review of air-coupled ultrasonic materials characterization. Ultrasonics 54:1804–1816
- Döring J, Bovtun V, Bartusch J, Erhard A, Kreutzbruck M, Yakymenko Y (2010) Nonlinear electro-mechanical response of the ferroelectret ultrasonic transducers. Appl Phys A Mater Sci Process 100:479–485
- Döring J, Bovtun V, Gaal M, Bartusch J, Erhard A, Kreutzbruck M, Yakymenko Y (2012) Piezoelectric and electrostrictive effects in ferroelectret ultrasonic transducers. J Appl Phys 112:084505. <https://doi.org/10.1063/1.4759052>
- Fang Y, Lin L, Feng H, Lu Z, Emms GW (2017) Review of the use of air-coupled ultrasonic technologies for nondestructive testing of wood and wood products. Comput Electron Agric 137:79–87
- Fuller J, Ross R, Dramm J (1994) Honeycomb and surface check detection using ultrasonic nondestructive evaluation. Res Note FPL-RN-0261 USDA For Service, For Prod Lab, Madison
- Gaal M, Bartusch J, Dohse E, Schadow F, Köppe E (2016a) Focusing of ferroelectret air-coupled ultrasound transducers. In: AIP conference proceedings, vol 1706, p 080001. <https://doi.org/10.1063/1.4940533>
- Gaal M, Bovtun V, Stark W, Erhard A, Yakymenko Y, Kreutzbruck M (2016b) Viscoelastic properties of cellular polypropylene ferroelectrets. J Appl Phys 119:125101. <https://doi.org/10.1063/1.4944798>
- Gaal M, Caldeira R, Bartusch J, Schadow F, Vössing K, Kupnik M (2019) Air-coupled ultrasonic ferroelectret receiver with additional bias voltage. IEEE Trans Ultrason Ferroelectr Freq Control 66(10):1600–1605. <https://doi.org/10.1109/TUFFC.2019.2925666>
- Gan TH, Hutchins DA, Green RJ, Andrews MK, Harris PD (2005) Noncontact, high-resolution ultrasonic imaging of wood samples using coded chirp waveforms. IEEE Trans Ultrason Ferroelectr Freq Control 52(2):280–288
- Hilbers U, Thoemen H, Hasener J, Frühwald A (2012) Effects of panel density and particle type on the ultrasonic transmission through wood-based panels. Wood Sci Technol 46:685–698
- Kabir MF, Schmoltdt DL, Schafer ME (2002) Time domain ultrasonic signal characterization for defects in thin unsurfaced hardwood lumber. Wood Fiber Sci 34(1):165–182

- Marchetti B, Munaretto R, Revel G, Tomasini EP, Bianche VB (2004) Non-contact ultrasonic sensor for density measurement and defect detection on wood. In: 16th World conference on nondestructive testing, Montreal, Canada, August 30th–September 3rd
- Marhenke T, Neuenschwander J, Furrer R, Zolliker P, Twiefel J, Hasener J, Wallaschek J, Sanabria S (2020) Air-coupled ultrasound time-reversal (ACU-TR) for subwavelength nondestructive imaging. *IEEE Trans Ultrason Ferroelectr Freq Control* 67(3):651–663. <https://doi.org/10.1109/TUFFC.2019.2951312>
- Ross RJ, Pellerin RF (2002) *Nondestructive evaluation of wood*. Forest Products Society, Madison
- Sanabria SJ (2012) *Air-coupled ultrasound propagation and novel non-destructive bonding quality assessment of timber composites*. Dissertation, ETH Zurich
- Sanabria SJ, Furrer R, Neuenschwander J, Niemz P, Sennhauser U (2013) Novel slanted incidence air-coupled ultrasound method for delamination assessment in individual bonding planes of structural multi-layered glued timber laminates. *Ultrasonics* 53:1309–1324
- Schafer M, Ross R, Brashaw B, Adams R (1999) Ultrasonic inspection and analysis techniques in green and dried lumber. Proceedings of the 11th international symposium NDT Wood, USDA For Prod Lab, Madison, pp 95–102
- Schmoldt DL, Duke, JC (Jr), Morrone M, Jennings CM (1994) Application of ultrasound nondestructive evaluation to grading pallet parts. In: Proceedings of the 9th international symposium NDT Wood, USDA For Prod Lab, Madison, pp 183–190
- Solodov I, Pfeleiderer K, Busse G (2004) Nondestructive characterization of wood by monitoring of local elastic anisotropy and dynamic nonlinearity. *Holzforschung* 58:504–510
- Tiitta M (2006) *Non-destructive methods for characterisation of wood material*. Dissertation, Kuopio University Publications C. Natural and Environmental Sciences 202. Kopijyvä, Kuopio
- Tiitta M, Beall FC, Biernacki JM (1998) Acousto-ultrasonic assessment of internal decay in glulam beams. *Wood Fiber Sci* 30:24–37
- Tiitta M, Biernacki JM, Beall FC (2001) Classification study for detecting internal decay in glulam beams by acousto-ultrasonics. *Wood Sci Technol* 35:85–96
- Tiitta M, Tomppo L, Möttönen V, Marttila J, Antikainen J, Lappalainen R, Heräjärvi H (2017) Predicting the bending properties of air dried and modified *Populus tremula* L. wood using combined air-coupled ultrasound and electrical impedance spectroscopy. *Eur J Wood Prod* 75:701–709. <https://doi.org/10.1007/s00107-016-1140-0>
- Tomppo L (2013) *Novel applications of electrical impedance and ultrasound methods for wood quality assessment*. Publications of the University of Eastern Finland. Dissertations in Forestry and Natural Sciences
- Tomppo L, Tiitta M, Lappalainen R (2014) Non-destructive evaluation of checking in thermally modified timber. *Wood Sci Technol* 48:227–238
- Tomppo L, Tiitta M, Lappalainen R (2016) Air-coupled ultrasound and electrical impedance analyses of normally dried and thermally modified Scots pine (*Pinus sylvestris*). *Wood Mater Sci Eng*. 11(5):274–282. <https://doi.org/10.1080/17480272.2014.983162>
- van Dyk H, Rice RW (2005) Ultrasonic wave velocity as a moisture indicator in frozen and unfrozen lumber. *For Prod J* 55(6):68–72
- Verkasalo E, Ross R, TenWolde A, Youngs RL (1993) Properties related to drying defects in Red Oak wetwood. Res Paper FPL-RP-516 USDA For Service, For Prod Lab, Madison, WI, USA
- Vössing K, Niederleithinger E (2018) Nondestructive assessment and imaging methods for internal inspection of timber. A review. *Holzforschung* 72:467–476
- Vössing K, Gaal M, Niederleithinger EK (2018) Air-coupled ferroelectret ultrasonic transducers for non-destructive testing of wood-based materials. *Wood Sci Technol* 52:1527–1538
- Vun RY, Bhardwaj MC (2004) Non-contact ultrasonic characterization of in-plane density variation in oriented strandboard. In: 16th World Conference on Nondestructive Testing, Montreal, Canada, August 30th–September 3rd
- Vun RY, Hoover K, Janowiak J, Bhardwaj MC (2008) Calibration of non-contact ultrasound as an online sensor for wood characterization: effects of temperature, moisture, and scanning direction. *Appl Phys A* 90(1):191–196